

Direct Measurement of the L/K Ratio in ${}^7\text{Be}$ Electron Capture

P. A. Voytas,¹ C. Ternovan,¹ M. Galeazzi,² D. McCammon,² J. J. Kolata,³ P. Santi,³ D. Peterson,³ V. Guimarães,³ F. D. Becchetti,⁴ M. Y. Lee,⁴ T. W. O'Donnell,⁴ D. A. Roberts,⁴ and S. Shaheen^{4,5}

¹Physics Department, Wittenberg University, Springfield, Ohio 45501-0720

²Physics Department, University of Wisconsin–Madison, Madison, Wisconsin 53706-1390

³Physics Department, University of Notre Dame, Notre Dame, Indiana 46556-5670

⁴Physics Department, University of Michigan, Ann Arbor, Michigan 48109-1120

⁵Physics Department, Faculty of Science, King Abdulaziz University, Jeddah, Saudi Arabia

(Received 24 May 2001; published 18 December 2001)

The ratio of L - to K -shell electron captures in light nuclei is particularly sensitive to electron overlap and exchange effects. Calculations of these effects in ${}^7\text{Be}$ disagree by more than 20%. We report a measurement of the L/K ratio in ${}^7\text{Be}$, using a cryogenic microcalorimeter which clearly separates L - and K -shell captures. The obtained L/K ratio of 0.040(6) is less than half that of existing predictions for free ${}^7\text{Be}$. The discrepancy is likely due to in-medium effects distorting the L -shell electron orbitals.

DOI: 10.1103/PhysRevLett.88.012501

PACS numbers: 23.40.–s, 27.20.+n, 29.40.Vj

Investigations of nuclear electron capture over the past 65 years have contributed to the development of the solar model [1], to tests of the Fermi theory of beta decay [2], and (to the extent that agreement with experiment is not obtained without correct atomic wave functions [3]) to tests of calculations of atomic wave functions. Knowledge of electron capture observables is important for certain searches for massive neutrinos [4] and for radionuclide metrology [5]. Our primary interest is in studying the weak interaction through electron capture experiments such as those described in Ref. [6]. For such experiments, a thorough understanding of atomic electronic effects on the decay is required. The ratio of electron captures from the L shell to those from the K shell (the L/K ratio) is particularly sensitive to the details of electronic wave functions of the initial and final states. Two current theoretical calculations of the L/K ratio in ${}^7\text{Be}$ differ by more than 20% [3].

Historically the L/K ratio has been measured by observing x rays or Auger electrons emitted during the deexcitation of the daughter atom. These indirect techniques have provided most of the data on electron capture but often involve many corrections, particularly to account for self-absorption, that become larger the lower the Z of the parent (and therefore the lower the x ray or Auger energy). Cryogenic microcalorimeters [7,8], which measure a temperature rise resulting from energy deposited by individual events that are fully contained within the detector, are well suited to measuring such low energy events [9] with good resolution and essentially unit efficiency. We report here the observation of electron capture in ${}^7\text{Be}$ (the lightest isotope to undergo electron capture) embedded in a cryogenic microcalorimeter. The resolution of the instrument [8.5(7) eV FWHM] clearly separates captures from the K and L shells, allowing for a first direct exploration of the L/K ratio in ${}^7\text{Be}$.

In order to understand the signals expected in a calorimeter from the decaying ${}^7\text{Be}$, we need to look in

some detail at the decay and detection process. When ${}^7\text{Be}$ decays, an electron from either the K or L shell can be captured by the nucleus to either the ground state or first excited state of the residual ${}^7\text{Li}$ nucleus. The neutrino emitted in this process escapes, and the residual nucleus recoils. For K capture resulting in a ${}^7\text{Li}$ nucleus in its ground state, a neutrino with an energy of 862 keV is emitted and the residual nucleus recoils with 57 eV of kinetic energy. In this case the ${}^7\text{Li}$ atom is left in a state with one K -shell and two L -shell electrons. The hole in the K shell subsequently fills and the K -shell binding energy (55 eV in bulk Be metal with respect to the Fermi energy [10]) will also be deposited as photons or Auger electrons. Both the recoil and rearrangement energies will contribute to the heating of the calorimeter, and since the processes happen on a time scale very short compared to the thermal time constant ($\tau \approx 10$ ms) of the calorimeter, the two energies add resulting in a total energy deposited for this event of 112 eV. L capture to the nuclear ground state of ${}^7\text{Li}$ also results in a recoil energy of 57 eV, but this event leaves the ${}^7\text{Li}$ atom in its ground state configuration so no further energy is released. In the above treatment and throughout this work we ignore the negligible differences in neutrino energy due to differences in binding energy of the captured electrons. Note also that if the ${}^7\text{Li}$ is left in any excited atomic state, the total energy deposited is the same as calculated above as long as the deexcitation/rearrangement happens on a time scale much shorter than the thermal time constant of the microcalorimeter.

In the case of capture to the first excited state of the ${}^7\text{Li}$ nucleus, the situation is more complicated due to the lifetime of the excited state and the nonzero time it takes the recoiling nucleus to stop. If, after emitting the neutrino, the ${}^7\text{Li}^*$ comes to rest before emitting the γ ray, then there is a unique total energy (equal to the sum of the recoil energies from each process plus any electronic rearrangement energy) deposited in the calorimeter. However, if the ${}^7\text{Li}^*$ is

still moving when the γ ray is emitted, the kinetic energy after γ -ray emission depends on the direction of emission with respect to the momentum of the ${}^7\text{Li}^*$ at the time the γ ray is emitted, leading to a range of total recoil energies. It appears from our data that the time for the recoil to come to rest is more than a factor of 3 larger than the γ -decay lifetime [73(2) fs [11]]. This is discussed below.

In our experiment the ${}^7\text{Be}$ was produced with the TWINSOL [12] radioactive beam facility at the University of Notre Dame. A 100 particle nA beam of ${}^6\text{Li}$ at 15 MeV was incident on a 2.54 cm long gas cell filled with one atmosphere of ${}^3\text{He}$, producing ${}^7\text{Be}$ via the ${}^3\text{He}({}^6\text{Li}, {}^7\text{Be})d$ reaction. Recoil ${}^7\text{Be}$ ions at a central energy of 8.5 MeV were brought to a focus 5.5 m downstream of the ${}^3\text{He}$ cell by two superconducting solenoids. The ${}^7\text{Be}$ flux and spatial distribution were measured with a position-sensitive silicon surface barrier detector to be 5×10^5 per second, uniform to within 50% over a 2.5 cm diameter circle. The flux detector was replaced with a target holder on which four samples of mercury telluride (HgTe) approximately $0.5 \text{ mm} \times 1 \text{ mm} \times 8 \mu\text{m}$ thick were mounted with adhesive. Mercury telluride was chosen for its low specific heat and its good thermalization properties. After implanting under these conditions for 44 h, the estimated activity in each chip was about 5 decays per second. The target holder was then immersed in a solvent and the mercury telluride chips floated off.

The activity in the chips was actually measured to be about 10 Hz by counting the 478 keV γ rays from the 10.52% branch to the first excited state of the ${}^7\text{Li}$ nucleus [11]. As this activity was too high to be used in the microcalorimeter (due to pulse pileup), the chips were cleaved to a size with an activity of 2 to 3 Hz. Four of the chips were mounted (Fig. 1) on microcalorimeters using Stycast 2850FT epoxy. The microcalorimeters were part of a 36 pixel array based on ion-implanted silicon Si:P:B thermistors that was developed for the x-ray quantum calorimeter sounding rocket program [13–15]. The array was installed in contact with the cold plate of an adiabatic demagnetization refrigerator and maintained at a temperature of 60 mK. The energy deposited in a

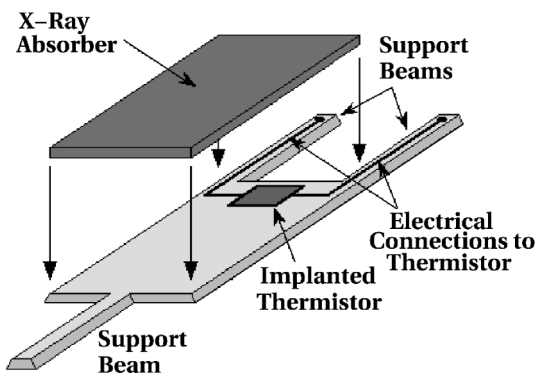


FIG. 1. Schematic depiction of the silicon microcalorimeter.

microcalorimeter by a decay event results in a small temperature rise. The resistance of the silicon-implanted thermistors is strongly dependent on the temperature. Using a constant bias current, the thermistors produce a voltage that varies with the microcalorimeter temperature. After each event, a weak thermal link to the refrigerator cold plate allows the temperature of the microcalorimeter to return to its original value with a time constant of about 10 ms. The voltages across the thermistors are preamplified using silicon junction field-effect transistor source followers operating at about 120 K, and further amplified by external low noise amplifiers. The output is sampled continuously by a 12 bit digitizer at $50 \mu\text{s}$ intervals, and for each event above a threshold of about 20 eV, a 4096 channel sample containing the pulse (Fig. 2) is written to tape for off-line analysis.

The calorimeters were calibrated using an external, α -excited fluorescence source with a Teflon target which provided carbon and fluorine K x rays at 277 eV and 677 eV, respectively. The monoenergetic events at 112 eV from the ${}^7\text{Be}$ K -shell capture to the ${}^7\text{Li}$ nuclear ground state provided information on gain drifts when the fluorescence source was removed.

The off-line analysis is as follows: the pulses are first digitally filtered to obtain the best signal to noise ratio on the amplitude. An estimate of the baseline noise of the system is obtained by once-per-second sampling of the output signals, independent of the 20 eV threshold. Signal pulses from the calibration source are averaged and Fourier transformed to obtain the expected signal shape. An optimum filter weights each frequency bin by the ratio of the complex conjugate of the average signal to the mean square of the noise in that bin. The pulse amplitude is then converted into energy using the scale determined from the calibration source. Gain drift is corrected using the observed amplitudes of the 112 eV K -capture line. Finally, cuts were applied to the pulse characteristics to eliminate

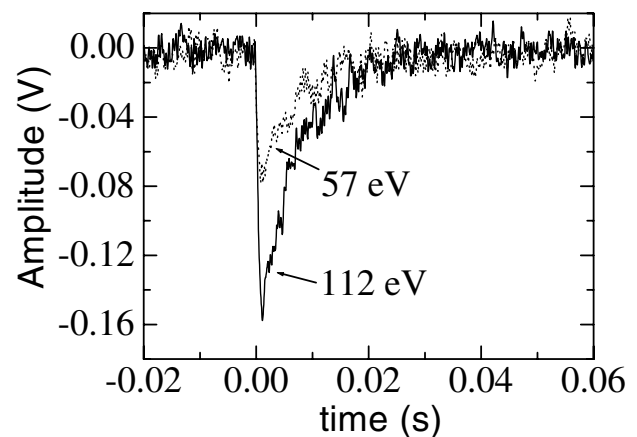


FIG. 2. Example pulses from the microcalorimeter showing noise levels and the characteristic time constant.

pileup. Particular care in the analysis has been dedicated to the identification of pileup events and double pulses. Pulses less than 150 ms apart were discarded. To check that residual pileup did not affect the results, the data have been acquired in two different runs, separated by 80 days. Since the half-life of ${}^7\text{Be}$ is 53.29(7) days [11], the activity of the samples was lower by about a factor of 3 in the second run. Separate analysis of the two runs shows no evidence of any statistically significant difference between the two spectra.

Of the four pixels on which samples were mounted, two were damaged in mounting, and one had relatively poor resolution. Therefore, data were obtained from only one pixel. The energy histogram (Fig. 3) of these data was fit to a spectrum consisting of Gaussian peaks with high-energy exponential tails for captures to the nuclear ground state, a numerically modeled component (taking into account the effects of a ${}^7\text{Li}^*$ emitting a γ ray while still moving) for the decays from the K and L shells to

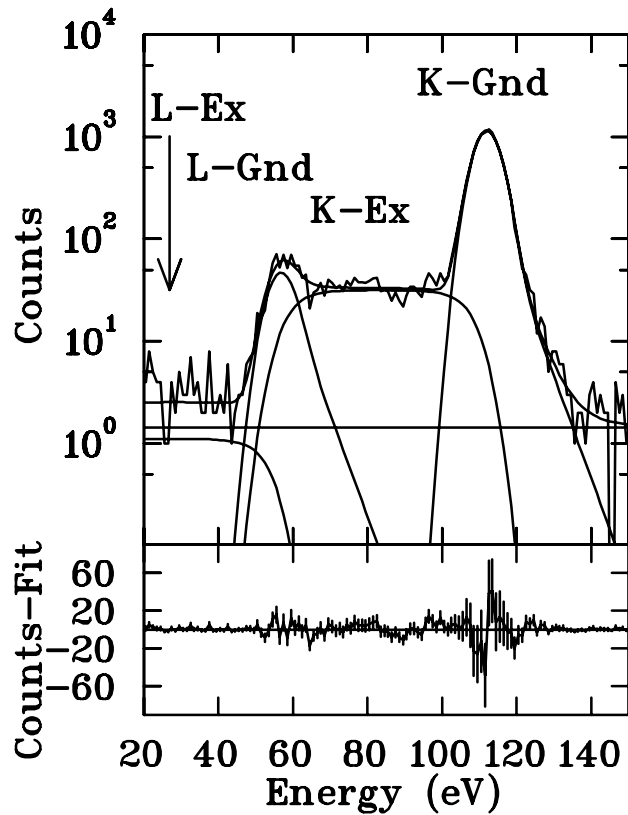


FIG. 3. Energy histogram of ${}^7\text{Be}$ electron capture events for the second set of data. The smooth curve is a fit as described in the text with individual contributions to the fit shown below it. The fit assumes linear momentum loss with time and the branching ratio to the first excited state of ${}^7\text{Li}$ was a free parameter. The peaks labeled K -Gnd and L -Gnd correspond to captures from the K or L shell, respectively, to the ground state of the ${}^7\text{Li}$ nucleus. The regions labeled K -Ex and L -Ex correspond to captures to the first excited state of the ${}^7\text{Li}$ nucleus. In the upper panel, the horizontal line near the value 1 represents the flat background.

the excited nuclear state, and a flat background. Among the free parameters of the fit was the width of the Gaussian peaks [8.5(7) eV FWHM] which is a measure of the energy resolution. Other parameters included the L/K ratio, the branching ratio, the area of the K -capture peak, the fraction of events in the high-energy tail, the decay constant of the high-energy tail, a flat background, mean energies of peaks, and a parameter quantifying the rate at which the recoils lose momentum.

As indicated above, the nonzero slowing time of the recoils and the lifetime of the nuclear excited state give a broad distribution of energies for decays to the first nuclear excited state of ${}^7\text{Li}$. Three models for the recoil slowing process were considered: a linear decrease in velocity over time, an exponential decrease in velocity over time, or a quadratic, concave down velocity vs time dependence. None of the models is completely realistic; however, their differing curvatures cover a range of possible behaviors. Each of the two runs was fit separately and each run was fit with each model twice: once with the branching ratio for the decay to the first excited state of the ${}^7\text{Li}$ nucleus fixed at the accepted value ($\lambda_{\text{ex}}/\lambda_{\text{tot}} = 0.1052$ [11]) and once with the ratio free to vary. The results of this procedure are summarized in Table I. Unweighted averaging of all fits yields an L/K ratio of 0.040(6) where the uncertainty represents the standard deviation of the distribution of values. Statistical uncertainties reported from the fitting program are less than one-tenth as large. Included in the table are the fit results for the slowing parameters of the model. While they vary considerably, the indication is that the rate of loss of momentum by the recoils is more than 3 times smaller than the γ -decay rate.

Theoretical predictions for the L/K capture ratio have been made (see Ref. [3] for an extensive review). The most naive prediction is just the probability ratio of L -shell to K -shell wave functions at the nucleus (0.0331 in beryllium

TABLE I. Results of fits to the recoil energy spectra of ${}^7\text{Be}$ decay. Various models of the recoil slowing were fit and the branching ratio to the first excited nuclear state of ${}^7\text{Li}$ was either a free parameter of the fit (upper set of numbers, $\nu = 109$) or fixed at the accepted value (lower set of numbers, $\nu = 110$). The slowing parameters are the ratio of the γ -decay rate (λ_g) to the rate of loss of momentum (λ_p). Each line represents an average over two separate data runs and three different slowing models. The range of slowing parameters and χ^2/ν reflects the variation with differing slowing models and data runs. The uncertainty in the L/K ratio and in the branching ratio represents the standard deviation of the distribution of values from the fits. “HE tail” refers to whether or not a high-energy tail is included in the peak shape. See text for additional details.

	L/K ratio	Branching ratio	Slowing parameter	χ^2/ν
HE tail	0.036(4)	0.095(12)	$\lambda_g/\lambda_p = 3-9$	1.1
No HE tail	0.0413(6)	0.123(14)	$\lambda_g/\lambda_p = 3-20$	1.7-1.9
HE tail	0.037(5)	0.1052	$\lambda_g/\lambda_p = 3-9$	1.1-1.5
No HE tail	0.046(3)	0.1052	$\lambda_g/\lambda_p = 3-5$	1.8-2.0

[16]). However, the occupancy of the electron states in the final ${}^7\text{Li}$ atom is affected by exchange and overlap effects of the parent and daughter electron clouds. Since our measurement includes the energy of rearrangement in the final state, we must expect to use an L/K ratio modified by these effects. Calculations using modern wave functions and techniques follow two basic theoretical approaches, one due to Vatai and another due to Bahcall. Both are reported in Ref. [3]. Bahcall's approach assumes closure to perform the sum over final atomic states, while Vatai's neglects some contributions involving shakeup or shakeoff. Bahcall's technique yields $L/K = 0.09$, whereas Vatai's gives $L/K = 0.11$ (both with no theoretical uncertainties reported). The dramatic difference from the naive L/K result applies only to ${}^7\text{Be}$ —the effects are much smaller in higher- Z systems.

Further complications arise due to the environment of the beryllium atoms when they undergo electron capture. The theoretical calculations mentioned above apply to free beryllium atoms. However, in our experiment, as in most, the ${}^7\text{Be}$ is in a solid host so considerable distortion of the outer electron wave functions is to be expected. Calculations of the change in probability density of the L -shell electrons at the beryllium nucleus have recently been carried out [17] to investigate lifetime changes of ${}^7\text{Be}$ in various chemical environments. These calculations, which do not include exchange and overlap corrections, indicate that the decay rate of ${}^7\text{Be}$ in a ${}^9\text{Be}$ host is 1.9% lower than free ${}^7\text{Be}$ and that variations for ${}^7\text{Be}$ in different hosts can change the decay rate by comparable amounts. The effect on the L/K ratio might be an order of magnitude larger since captures from the L shell in free ${}^7\text{Be}$ would make up only about 1/10 of total decays. The chemical environment is also expected to alter the exchange and overlap effects, which could have an additional large effect on the L/K ratio.

In conclusion, we have performed the first-ever measurement of the L/K capture ratio in the decay of ${}^7\text{Be}$. The value we obtain is relatively independent of which of three quite different slowing-down models is used in accounting for the branch to the nuclear excited state of ${}^7\text{Li}$. This is an indication of the robustness of our result. We have also determined that the time scale for the slowing down of the recoil ${}^7\text{Li}$ in the HgTe medium has a lower limit of about 210 fs. Our experimental value for the L/K ratio is a factor of about 2 lower than the average of existing theoretical predictions for free beryllium. The disagreement is most likely due to the solid-state effects mentioned above. Given the present level of uncertainty in treating

these environmental effects, it appears that a more meaningful comparison with theoretical predictions must await a more thorough understanding of the effects of the host material on the beryllium atomic wave function. However, it is clear that cryogenic microcalorimeters offer an exciting new tool for the measurement of low-energy decay phenomena. Their resolution and efficiency allow for measurements to be made with unprecedented accuracy, and the technique offers much promise in applications such as described in this Letter.

This work was supported in part by Wittenberg University, the McGregor Fund, and NSF Grants No. 99-01133 and No. 98-04869.

-
- [1] J. N. Bahcall, *Astrophys. J.* **467**, 475 (1996).
 - [2] H. Yukawa and S. Sakata, *Phys. Rev.* **51**, 677 (1937).
 - [3] W. Bambynek *et al.*, *Rev. Mod. Phys.* **49**, 77 (1977); **49**, 961 (1977).
 - [4] F. X. Hartmann, *Phys. Rev. C* **45**, R900 (1992).
 - [5] E. Schönfeld, *Appl. Radiat. Isot.* **49**, 1353 (1998).
 - [6] L. M. Folan and V. I. Tsifrinovich, *Phys. Rev. Lett.* **74**, 499 (1995).
 - [7] S. H. Moseley, J. C. Mather, and D. McCammon, *J. Appl. Phys.* **56**, 1257 (1984).
 - [8] C. K. Stahle, D. McCammon, and K. D. Irwin, *Phys. Today* **52**, No. 8, 32 (1999).
 - [9] F. Fontanelli *et al.*, *Nucl. Instrum. Methods Phys. Res., Sect. A* **370**, 273 (1996).
 - [10] R. Firestone, Virginia S. Shirley, Coral M. Baglin, and S. Y. Frank Chu, *The 8th Edition of the Table of Isotopes* (John Wiley & Sons, Inc., New York, 1998), p. F-37.
 - [11] F. Ajzenberg-Selove *et al.*, *Nucl. Phys.* **A490**, 1 (1988). Information extracted from the ENSDF database revision of 5-Sep-2000, using the NNDC Online Data Service.
 - [12] M. Y. Lee *et al.*, *Nucl. Instrum. Methods Phys. Res., Sect. A* **422**, 536 (1999).
 - [13] M. Galeazzi, D. McCammon, and W. T. Sanders, in *X-ray and Inner-Shell Processes*, edited by R. W. Dunford, D. S. Gemmell, E. P. Kanter, B. Krässig, S. H. Southworth, and L. Young, AIP Conf. Proc. No. 506 (AIP, Melville, NY, 2000), p. 638.
 - [14] F. S. Porter *et al.*, *Nucl. Instrum. Methods Phys. Res., Sect. A* **444**, 175 (2000).
 - [15] R. L. Kelley *et al.*, *Nucl. Instrum. Methods Phys. Res., Sect. A* **444**, 170 (2000).
 - [16] D. R. Hartree and W. Hartree, *Proc. R. Soc. London A* **150**, 9 (1935).
 - [17] A. Ray *et al.*, *Phys. Lett. B* **455**, 69 (1999).